NASA Technical Paper 2076
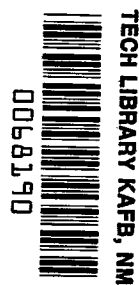
October 1982

Characterization of Soil and Postlaunch Pad Debris From Cape Canaveral Launch Complex and Analysis of Soil Interaction With Aqueous HCl
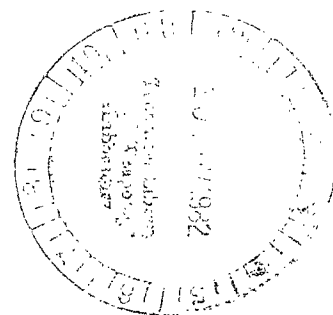
G. L. Pellett,
L. W. Spangler,
R. W. Storey, Jr.,
and R. J. Bendura

NASA

Characterization of Soil and Postlaunch Pad Debris From Cape Canaveral Launch Complex and Analysis of Soil Interaction With Aqueous HCl
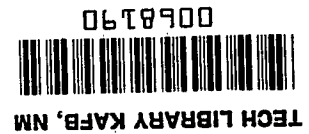
G. L. Pellett
Langley Research Center
Hampton, Virginia

L. W. Spangler
Kentron International, Inc.
Hampton, Virginia

R. W. Storey, Jr.,
and R. J. Bendura
Langley Research Center
Hampton, Virginia

SUMMARY

Soil samples, collected 0.5 to 3 km from the Titan III Launch Complex 40 at Cape Canaveral, Florida, were fractionated and analyzed in order to assess the physical and chemical interactions of entrained soil with solid-rocket exhaust clouds containing HCl. The sandy soil consisted primarily of quartz (silica) particles, 30 to 500 μm in diameter, but the larger-size fractions also contained several percent of seashell fragments. Differential and cumulative soil-mass size distributions are presented along with estimated sedimentation lifetimes, mineralogy, elemental compositions, and solution pH histories obtained during sequential titration of soil-fraction slurries with aqueous HCl. About 90 percent of the soil mass consisted of particles with a diameter greater than 165 μm. Initially, all fractions were slightly alkaline. Characteristic reaction times with HCl(aq) varied from a few minutes to several days, and capacities for reaction under acidic conditions varied from >10 to >40 g HCl/kg soil, depending on particle size. Airborne lifetimes of particles greater than 165 μm are conservatively less than 30 min, and this major grouping is predicted to represent a small short-term chemical sink for HCl (5 percent of total HCl). The smaller and more minor fractions (less than 10 percent with a diameter less than 165 μm) must also be considered, since they may act as giant cloud condensation nuclei (larger than 50 μm) over much longer airborne lifetimes, and with decreasing size their reactive capacity increases in both rate and extent. Finally, the demonstrated time dependency of neutralization (or buffering) is a complicating factor. This time-dependent neutralization not only influences the ability to deduce in-cloud HCl scavenging with reaction prior to dry or wet deposition but it also affects the accuracy of measured chemical compositions of near-field wet deposition occurring during the first few minutes and lasting up to several hours. Thus, for several reasons, entrained-soil particles can influence the composition and environmental impact of solid-rocket exhaust clouds.

INTRODUCTION

Large, but very imprecisely known, quantities of sandy soil (e.g., 10 to 50 metric tons) at the Air Force Cape Canaveral launch sites for Titan III are entrained into each solid-rocket-motor (SRM) exhaust cloud and then transported downwind until dry or wet deposition occurs. The entrainment initially occurs as a result of high-velocity plume impingement in the pad-flame trench area, and it subsequently occurs as a result of high surface winds characterized as "fire storm" convective effects. (See ref. 1.) The entrained-soil particles in the dry state will coagulate and scavenge alumina-exhaust particles. (See ref. 2.) Simultaneously, they will settle at relatively high rates, compared with the smaller alumina particles, thus leading to readily measurable dry or wet deposition downwind. (See refs. 3 to 6.) The sedimentation rate depends on particle agglomerate size, density, and shape. The soil particles can also serve effectively as giant cloud condensation nuclei (refs. 7 and 8), and they may react chemically; that is, they may scavenge and react with gaseous and aqueous HCl aerosol during sedimentation, and then react further with available acid after wet deposition. Significant adsorption occurs even in the case of quartz (silica) particles. (See refs. 9 to 11.)

The present paper provides basic data on these soil particulates and an assessment of the principal physical and chemical processes that occur during and after a launch. Specifically, it summarizes efforts to (a) characterize, with a gravimetric sieving technique, the size distributions of Cape Canaveral soil and a postlaunch-pad-debris sample, both of which were obtained near a Titan III Launch Complex (LC-40), and to (b) measure the neutralizing capacities of classified soil particle fractions by titration of aqueous suspensions with HCl. The data are then used to assess differential particle settling, particle size and time-dependent reaction effects in aqueous HCl, and the probable overall effects of soil particulates in Titan III SRM exhaust clouds. Although some of the aforementioned results were summarized recently in conjunction with other chemical studies of the soil and silica samples (ref. 12), the present paper documents the complete set of results obtained by the Langley Research Center.

SYMBOLS

d_p soil particle diameter

d_s sieve mesh size

F_m cumulative mass fraction

m(HCl)   molarity of aqueous HCl, mole HCl/liter

pH   measure of acidity due to $H^+(aq)$; defined for an idealized solution of fully dissociated HCl(aq) by $\log_{10}[1/m(HCl)]$

ΔX_m incremental mass fraction

ρ_p particle density

Abbreviations:

KSC   Kennedy Space Center

LC-40   Launch Complex 40

SRM   solid rocket motor

COLLECTION AND FRACTIONATION OF SOIL SAMPLES

Representative samples of the topmost layer of sandy soil and also a postlaunch-pad-debris sample were collected at Cape Canaveral, Florida, in the vicinity of the Titan III launch site, LC-40. The soil samples (denoted as KSC) were obtained during monitoring activities of Titan III exhaust effluents on March 11-12, 1975, for soil and on August 20, 1977, for pad debris. Three of the four soil samples were taken approximately downstream of the horizontal flame trench, and the fourth was collected 3 km to the south, outside the influence of the flame trench. Soil samples were obtained by scraping the top few millimeters of an unobstructed flat 3-m^2 area. Soil sample 1 was taken approximately 550 m from the LC-40 pad in an ENE direction at 70° from due north. Soil samples 2 to 4 were obtained at the following locations: 790 m

at 73°, 700 m at 65°, and 2930 m at 180°, respectively. All the soil samples are believed to contain locally dredged river soil that was originally used in the early 1960's to build up the outer-cape launch-complex areas (according to communication with Clair W. Bemiss of the Kennedy Space Center). Soil sample 1 is considered, because of its location, the most representative of the surface soil and accumulated debris which typically becomes airborne during a launch from LC-40 as the result of flame-trench plume-impingement and cloud rise dynamics. For this reason, particle-size distributions and acid titrations with pH measurements were focused primarily on soil sample 1.

The pad-debris sample was obtained by postlaunch vacuuming of a preselected 3-m^2 area, on the concrete pad of LC-40, which had been vacuumed clean just prior to launch. The purpose of the pad sample was to provide a first characterization of the airborne debris which typically deposits in the immediate vicinity of the launch site.

Each soil and pad-debris sample was classified into 14 size categories by using a multistage calibrated-screen sifting technique (a sonically vibrated sifter). Two sequential multiscreen processing steps, each several minutes long, were used to classify the larger- and smaller-size groupings. The subsamples retained on each screen were transferred to weighing paper, massed on an analytical balance, and then photomicrographed. Conservation of sample mass was demonstrated after fractionation.

RESULTS

Characterization of Fractions

The resulting raw-mass-retention data for KSC soil sample 1 are shown on a log-log plot in figure 1. Note that for sieve mesh size d_s, the logarithmic size-interval spacings for $d_s \geqslant 149$ μm differ from that for $d_s < 149$ μm. This was a characteristic of the screen set used.

Results of an independent fractionation and mineralogical analysis of sample 2 are shown in table I. (See refs. 9, 10, and 12.) The sample is obviously hetero-geneous in composition since it consists of quartz, mica, feldspar, heavy minerals, organic matter, and clay. The particle sizes range from smaller than 2 μm to larger than 1000 μm. It is noted that 88 percent of the medium-sand fraction is quartz. Significant quantities of seashell fragments were also observed in the fine-to-coarse particle-size fractions.

Power-Law Cumulative Soil-Mass Distributions

The distributions for normalized cumulative mass fraction F_m for soil sample 1 and the postlaunch-pad-debris sample are plotted on log-log coordinates in figure 2. Simple straight-line power-law fits are shown to be accurate representations of F_m as a function of particle diameter d_p over the range of 37 μm $\leqslant d_p \leqslant$ 200 μm, but they are totally inadequate for $d_p >$ 200 μm. For soil sample 1 only about one part in 10^4 (by mass) is smaller than 37 μm. The comparable mass abundance for postlaunch pad debris is one part in 250. Photomicrographs of the pad-debris sample contained in the final sift bag ($d_p < 37$ μm) indicated a large portion of alumina-like spheres ($\approx$50 percent by number) which fell almost exclusively within the size range from 5 to 20 μm. (Smaller spheres attached to soil particles were also observed but were not included in the 50 percent estimate.) The observed difference between the

TABLE I.- FRACTIONATION AND MINERALOGICAL ANALYSIS OF THE
SAND FRACTION OF SAMPLE 2[a]

(a) Fractionation analysis

[The most active fraction is the organic matter
  and clay. The clay is composed of 2:1 inter-
  stratified minerals such as kaolinite, gibbsite,
  and quartz]

Fraction	Size range, μm	Weight, percent
Organic matter		0.53
Clay	<2	.04
Silt	50 to 2	1.01
Very fine sand	105 to 50	1.79
Fine sand	250 to 105	32.86
Medium sand	500 to 250	51.97
Coarse sand	1000 to 500	11.03
Very coarse sand	>1000	.77
Total		100.00

(b) Mineralogical analysis

[Heavy minerals are minerals with a specific gravity greater
  than 2.86. They include epidote, hornblende, zircon,
  apatite, tourmaline, magnetite, and ilmenite]

Size range, μm	Mineral	Content, percent
500 to 250	Quartz	88
	Mica	5
	Heavy minerals	6
	Other	1
105 to 50	Quartz	60
	Feldspar	6
	Mica	2
	Heavy minerals	32

[a]Data were obtained from references 9, 10, and 12 after
soil sample 2 was split for analysis.

respective F_m values at $d_p < 100$ µm is consistent with the presence of SRM-derived alumina in the postlaunch-pad-debris sample.

Log-Parabolic Differential and Cumulative Soil-Mass Distributions

Since detailed calculations of soil-particle sedimentation with coagulation require a comprehensive characterization of the mass-size distribution extending beyond 200 µm, the data on all four soil samples were analyzed to find a satisfactory average-distribution function. Recall first that the raw data in figure 1 are not normalized to mass fraction and, furthermore, do not represent a consistent differential distribution since the sieve-size interval changed at 149 µm. Thus, the incremental mass-retention data on all four soil samples were first normalized to incremental mass fraction retained per unit of logarithmic size interval Δd_p, which originally applied for $d_p < 149$ µm, and is expressed as

$$\Delta d_p = \left(\sqrt[4]{2} - 1 \right) d_p \tag{1}$$

The resultant normalized differential mass-fraction data for all four soil samples are shown in figure 3. The collective data for the two or three smallest particle-size fractions suggest that there is an apparent curvature or "tailing" in the data. Since this tailing can be considered (a) consistent with a log-normal distribution, (b) the beginning of a transition to the smaller particle mode of a bimodal distribution, or (c) due to systematic experimental error, a simple log-parabolic distribution function was chosen to fit the data initially. Therefore, a trial-and-error best-fit normalized function is faired through the data in figure 3, and the corresponding expression for incremental mass fraction of soil ΔX_m, with particle size between d_p and $d_p + \Delta d_p$, is given by

$$\log_{10} \left[\Delta X_m \right] = \log_{10} \left[\left(\sqrt[4]{2} - 1 \right) d_p \frac{\Delta X_m}{\Delta d_p} \right] = a + bz + cz^2 \tag{2a}$$

where $z = \log_{10} \left(d_p / 1 \text{ µm} \right)$, which is nondimensional, and

$a = -37.78$

$b = 30.89$

$c = -6.44$

It can be shown that equation (2a) reduces to the differential form when $\lim \Delta X_m \to 0$. Thus,

$$dX_m = \frac{2.3026}{\sqrt[4]{2} - 1} 10^{a+bz+cz^2} dz \tag{2b}$$

The corresponding normalized cumulative mass fraction of soil with particle diameters $\leqslant d_p$ is then defined by the integral of equation (2b):

$$F_m = \int_0^{d_p} dX_m \qquad (3)$$

An examination of data fit in figure 3 indicates some relatively small but noticeable differences among the samples and also the possible need for a higher-order function such as log-normal or log-cubic in order to achieve an improved fit, especially if more extensive data are available. Presently, however, the characterization is considered adequate for the applied problem in view of other large uncertainties, such as the initial vertical distribution of entrained soil mass aloft and the variability and complexity of chemical properties as a function of size.

The normalized cumulative mass-distribution data for all four soil samples are plotted in figure 4, and the data are faired with the integrated log-parabolic distribution function (eq. (3)) deduced from analysis of figure 3. Again, the data on different soil samples deviate somewhat, and the fit with equation (3) could probably be improved upon as previously discussed.

Finally, the cumulative sonic-sifter data in figure 4 can be compared with the independently obtained results for sample 2 shown earlier in table I. For $d_p \geqslant 150$ μm, the data in figure 4 agree closely with an interpolation of the tabulated results, with both accounting for ≈ 93 percent of the total mass. However, the present data indicate a mass fraction for particles of $d_p \leqslant 50$ μm (0.025 percent), which is considerably smaller than that shown in table I (1.05 percent if neglecting organic matter). These differences could have stemmed from uneven division of the original bulk sample, subsequent handling, and also the initial aqueous-peroxide-oxidation and drying step that was used to assay organic matter in the data in table I prior to fractionation.

Sedimentation of Entrained Soil Mass

Now that the probable initial distribution of entrained soil mass has been defined, it is possible to characterize the distribution of soil-particle lifetimes in an SRM exhaust cloud that are a result of any assumed initial condition. Sedimentation rates for spherical particles of specified density, falling at terminal velocity in air at 21°C and atmospheric pressure, were read graphically from reference 13. These were originally calculated from Stokes law for particles in the size range of $10 \leqslant d_p \leqslant 40$ μm, and from an intermediate transition expression (to Newton's law) for particles in the size range of $40 < d_p \leqslant 1000$ μm.

A characteristic settling time, which is equivalent to the airborne lifetime, was, thus, calculated for spherical particles having a density of 2 and 3 g/cm³ that were falling 1000 m in still air. The results, shown in figure 5, indicate a large and significant variation in settling time for the particle range of interest. For example, when $d_p \geqslant 200$ μm the settling time will be less than 15 min, provided the following conditions are accepted: (a) 1000 m as a reasonable average initial height for the ground-debris portion of the altitude-stabilized SRM exhaust cloud, and (b) an equivalent spherical particle density which ranges from 2 to 3 g/cm2. For smaller particles, the settling or residence time becomes increasingly significant, especially with respect to cloud microphysics and chemical-reaction processes with substantial

downwind transport. Some examples are 30 min for 100 μm, 1 hr for 65 μm, 2 hr for 44 μm, and 4 hr for 30 μm.

Although detailed calculations for sedimentation with coagulation have not been made, the present results are adequate for defining the following logical set of conclusions with regard to the lifetime and distribution of entrained soil in SRM exhaust clouds: (1) Sedimentation and coagulation processes (which form agglomerates from supermicron particles mostly by inertial impaction and from submicron particles by Brownian diffusion) should lead to deposition of nearly all the entrained-soil mass during the first 2 hours after launch in the absence of strong updrafts; (2) the distributions of soil particles in the SRM cloud, below it, and depositing on the ground will be significantly different at any given time and will change rapidly with time; and (3) the distribution of soil particles differs greatly from that of alumina-exhaust particulates, which tend to exhibit discrete modes at roughly 0.01 μm (fine-particle, high-temperature condensation mode; particles will coagulate rapidly), 0.1 μm (accumulation mode), and 1 to 2 μm (coarse-particle mode). (See refs. 7, 8, 14, and 15.) The observed alumina spheres of 5 to 20 μm in the postlaunch-pad-debris sample are relatively rare in SRM exhaust (in terms of relative number and mass) but nevertheless constitute a fourth coarse-particle mode for the alumina.

Soil Elemental Composition

Elemental bulk composition data were obtained on all four soil samples with a standard neutron-activation-analysis technique developed and applied by A. K. Furr of Virginia Polytechnic Institute and State University. (See ref. 16.) The compositions in units of parts per million (ppm) by mass are summarized in table II for all the measurable elements. The relatively large values for calcium are consistent with the visual (including microscopic) appearance of significant numbers of seashell fragments in virtually all the samples and fractionated subsamples. These seashell fragments, which are known to consist mostly of calcium carbonate along with lesser quantities of magnesium and other metal carbonates, can provide a significant neutralization capacity for HCl.

Titration of Soil Slurries with Aqueous HCl

Selected fractions of soil sample 1, in quantities ranging from 0.1 to 2 g, were slurried in 100 ml of distilled water and titrated incrementally with 0.05 molar HCl. A pH electrode was used to monitor the continuously stirred slurries. Initially, a preselected minimum reaction time of 10 min was used between each rapid addition of aqueous HCl and the recording of pH. As shown in the titration history of the largest particle-size sample investigated (250 μm < d_p < 354 μm) in figure 6(a), it soon became apparent that a slow buffering process was occurring. Thus, the "standard" sequence of rapid incremental titrations, each followed by a 10-min stirred reaction time, was altered periodically to allow for longer times of specified, but variable, duration. Titration was then resumed after each prescribed interval. Asymptotic "recoveries" to quasi-steady pH values required much longer than 10 min, and the resulting excursions in pH were sometimes very large. Figure 6(b) presents the results obtained from the 149 μm < d_p < 190 μm fraction, which had a significantly lower neutralization capacity than the larger particles in figure 6(a). Results for other selected fractions are shown in figures 6(c) to 6(e).

[Si, O, N, and C were not detectable by this technique
and, thus, are not included here]

Element	Concentration, ppm (g/g), found in soil sample –			
	1	2	3	4
Al	3 410	1 810	3 050	1 790
As	1.24	1.38	1.20	.41
Au	.017	.005	.009	.014
Ba	98	26	51	10
Br	2.67	2.37	2.53	1.20
Ca	29 900	63 700	29 300	20 500
Cd				.65
Ce	75	15.5	42	6.4
Cl		86	113	
Co	1.24	.53	.71	.41
Cr	51	28.7	53.7	22.3
Cs	.26	.24	.15	.15
Cu	16.6	18.5	18.9	17.5
Eu	.34	.23	.30	.081
Fe	3 230	1 940	2 610	1 410
Hf	16.2	5.33	11.2	1.46
Hg				.010
I		5	1.2	
K	465	292	366	292
La	21.9	5.39	11.7	1.77
Lu	0.28	0.098	0.12	0.049
Mg	350	1 091	971	489
Mn	82.6	29.2	72.2	16.2
Mo	1.9	1.7	1.5	.49
Na	522	659	1 073	410
Rb	12.8	3.1	7.5	3.5
Sb	.21	.36	.17	.087
Sc	.80	.38	.61	.23
Se	1.4	3.6	4.4	.21
Sm	4.8	1.42	2.86	.43
Sr	129	358	137	146
Ta	.91	.28	.33	.056
Th	19.4	2.5	11.0	1.04
Ti	2 540	631	1 470	155
U	2.5	1.0	1.3	.33
V	12.3	5.2	9.0	3.6
W	.81	.54	.69	.15
Yb	1.6	.56	.85	.21
Zn	34	20.3	27.2	26.2

Initial observations which apply to all five fractions investigated, extending down to $d_p > 88$ μm, are presented as follows: The soil was slightly alkaline. Initial pH's for corresponding size fractions (given in parentheses) were: 9.1 (for 354 to 250 μm), 8.6 (for 190 to 149 μm), 8.2 (for 149 to 125 μm), 7.6 (for 125 to 105 μm), and 7.2 (for 105 to 88 μm). The soil also exhibited a significant capacity to neutralize HCl. This capacity varies with particle size. The time dependence of neutralization and buffering reactions, which led to pH "recovery" over various extended reaction times, was most pronounced for the largest fraction but was still significant for the smallest fraction investigated.

One useful measure of soil-neutralization capacity, which has some significance in relation to the deposition of highly acidic rain from SRM exhaust clouds (refs. 17 to 19), is the ability of soil particles to raise the pH of a strongly acidic solution to a more moderate acidity condition, such as pH = 3. By accounting for the 2 ml of titrant required to acidify the initial water to pH = 3, neutralization capacities corresponding to relatively long reaction times were estimated as follows for various fractions: >40 g HCl/kg soil (for 354 to 250 μm); 14 g HCl/kg soil (for 190 to 149 μm); 18 g (for 149 to 125 μm); 22 g (for 125 to 105 μm); and 40 g (for 105 to 88 μm). A plot of these approximate results suggests that a broad minimum in neutralization capacity exists at about 200 μm (for 13 g HCl/kg soil, estimated), with particles in the vicinities of >300 μm and <100 μm having substantially higher capacities as defined previously. Since the initial slurry pH also decreased most rapidly over the size range from 190 to 88 μm, the combined results suggest a transition in the composition of neutralizing components for the smaller-size fractions.

If it is now assumed, in the absence of more complete data, that there is an average transient capacity of 20 g HCl/kg soil, and this assumption is combined with the previous estimates of entrained-soil mass (10 to 50 metric tons) and of HCl source strength up to 2-km altitude (20 metric tons, upper limit), a potential neutralization by soil particles of 1 to 5 percent of the total HCl in the Titan III ground cloud could occur.

SUMMARY OF RESULTS

Soil samples collected at various distances from the Titan III Launch Complex 40 at Cape Canaveral, Florida, consisted primarily of quartz particles, 30 to 500 μm in diameter, but the larger-size fractions also contained seashell fragments. The calcium content of the samples was appreciable (2 to 6 percent) based on the neutron-activation-analyses measurements.

The basicity characteristics of soil fractions covering the particle-size range from 350 to 90 μm were demonstrated by titration of aqueous slurries with 0.05 molar HCl. Initially, all the fractions were slightly alkaline. Characteristic reaction times, and capacities for reaction under acidic conditions, were both significant and variable with size. With decreasing size, long-term reaction capacity to pH = 3 attained a broad minimum of 13 g HCl/kg soil, centered at ≈200 μm. Since the reaction capacities of particles smaller than 190 μm increased systematically to ≈40 at 105 to 90 μm, whereas the initial slurry pH decreased from 8.6 to 7.2, a transition in the composition of neutralizing components occurred for these fractions. For a major portion of the soil (>90 percent by mass for >165 μm), the basicity characteristics in aqueous phase appear to be dominated by calcium-containing seashell fragments.

Total airborne lifetimes of exhaust-entrained soil particles greater than 165 μm are conservatively less than 30 min. Since adsorption of HCl and H_2O will occur, followed by vapor condensation and reaction with HCl(aq), which is known to be present in a young SRM exhaust cloud, this major fraction would represent a small but measurable (≤5 percent) short-term chemical sink for HCl. Additional removal of attached excess HCl(aq) would effectively increase this percentage. However, the possible roles of the smaller (<10 percent by mass for <165 μm) minor fractions must also be considered. Their airborne lifetimes become progressively longer, adsorption of HCl and water will significantly increase their potential activity as giant cloud condensation nuclei (>50 μm), and their subsequent aqueous reactivity per unit of mass tends to increase in both rate and extent.

CONCLUDING REMARKS

The present differential and cumulative soil-mass size distributions, sedimentation lifetimes, mineralogy, elemental compositions, and HCl titration results constitute some of the basic information needed to assess Kennedy Space Center soil interactions in solid-rocket-motor (SRM) clouds, provided that an initial vertical distribution of entrained-soil mass is specified. With respect to the rate and extent of chemical reactions with aqueous HCl, the demonstrated time dependency of neutralization and buffering is a complication factor. This time-dependent neutralization not only influences the ability to deduce HCl scavenging with reaction prior to dry or wet deposition but it also significantly affects the accuracy of measured chemical compositions of near-field wet deposition occurring during the first few minutes and lasting up to several hours.

Langley Research Center
National Aeronautics and Space Administration
Hampton, VA 23665
September 13, 1982

REFERENCES

1. Vander Arend, P. C.; Stoy, S. T.; and Kranyecz, T. E.: Feasibility Study of Launch Vehicle Ground Cloud Neutralization. NASA CR-145000, 1976.

2. Hwang, BaoChuan; and Gould, Robert K.: Rocket Exhaust Ground Cloud/Atmospheric Interactions. NASA CR-2978, 1978.

3. Gregory, Gerald L.; and Storey, Richard W., Jr.: Effluent Sampling of Titan III C Vehicle Exhaust. NASA TM X-3228, 1975.

4. Wornom, Dewey E.; and Woods, David C.: Effluent Monitoring of the December 10, 1974, Titan III-E Launch at Air Force Eastern Test Range, Florida. NASA TM-78735, 1978.

5. Bendura, Richard J.; and Crumbly, Kenneth H.: Ground Cloud Effluent Measurements During the May 30, 1974, Titan III Launch at the Air Force Eastern Test Range. NASA TM X-3539, 1977.

6. Steward, Roger B.; Sentell, Ronald J.; and Gregory, Gerald L.: Experimental Measurements of the Ground Cloud Effluents and Cloud Growth During the February 11, 1974 Titan-Centaur Launch at Kennedy Space Center. NASA TM X-72820, 1976.

7. Bollay, Eugene; Bosart, Lance; Droessler, Earl; Jiusto, James; Lala, G. Garland; Mohnen, Volker; Schaefer, Vincent; and Squires, Patrick: Position Paper on the Potential of Inadvertent Weather Modification of the Florida Peninsula Resulting From the Stabilized Ground Cloud. NASA CR-151199, 1976.

8. Bollay, Eugene; Bosart, Lance; Droessler, Earl; Jiusto, James; Lala, G. Garland; Mohnen, Volker; Schaefer, Vincent; and Squires, Patrick: Position Paper on the Potential of Inadvertent Weather Modification of the Florida Peninsula Resulting From Neutralization of Space Shuttle Solid Rocket Booster Exhaust Clouds. NASA CR-3091, 1979.

9. Kang, Yoonok; and Wightman, James P.: Adsorption of Hydrogen Chloride on Microcrystalline Silica. NASA CR-158018, 1979.

10. Skiles, Jean Ann; and Wightman, James P.: Characterization of the Adsorption of Water Vapor and Chlorine on Microcrystalline Silica. NASA CR-158100, 1979.

11. Kang, Yoonok; Skiles, Jean Ann; and Wightman, J. P.: Interaction of Gaseous Hydrogen Chloride and Water With Oxide Surfaces. 2. Quartz. J. Phys. Chem., vol. 84, no. 12, June 12, 1980, pp. 1448-1453.

12. Kang, Yoonok; Pellett, G. L.; Skiles, Jean Ann; and Wightman, J. P.: Interaction of Gaseous Hydrogen Chloride and Water With Sandy Soil. J. Colloid & Interface Sci., vol. 75, no. 2, June 1980, pp. 313-321.

13. Perry, John H., ed.: Chemical Engineers' Handbook, Third ed. McGraw-Hill Book Co., Inc., 1950.

14. Woods, D. C.: Rocket Effluent Size Distributions Made With a Cascade Quartz Crystal Microbalance. Proceedings of the 4th Joint Conference on Sensing of Environmental Pollutants, American Chem. Soc., c.1978, pp. 716-718.

15. Chaun, R. L.; and Woods, D. C.: Morphology and Elemental Composition Analysis by Size of Rocket Particulate Effluent. Conference Proceedings - 4th Joint Conference on Sensing of Environmental Pollutants, American Chem. Soc., c.1978, pp. 610-613.

16. Lenihan, J. M. A.; and Thomson, S. J., eds.: Activation Analysis - Principles and Applications. Academic Press, Inc., 1965.

17. Pellett, G. L.: Analytic Model for Washout of HCℓ(g) From Dispersing Rocket Exhaust Clouds. NASA TP-1801, 1981.

18. Pellett, G. L.; Sebacher, D. I.; Bendura, R. J.; and Wornom, D. E.: HCl in Rocket Exhaust Clouds: Atmospheric Dispersion, Acid Aerosol Characteristics, and Acid Rain Deposition. [Preprint] 80-49.6, Air Pollut. Control Assoc., June 1980.

19. Pellett, G. L.; Bendura, R. J.; and Storey, R. W.: Near-Field Deposition of Acidic Droplets from Titan III and Space Shuttle Launches. 1981 JANNAF Safety & Environmental Protection Subcommittee Meeting, CPIA Publ. 348 (Contract N00024-81-C-5301), Johns Hopkins Univ., Nov. 1981, pp. 259-266.
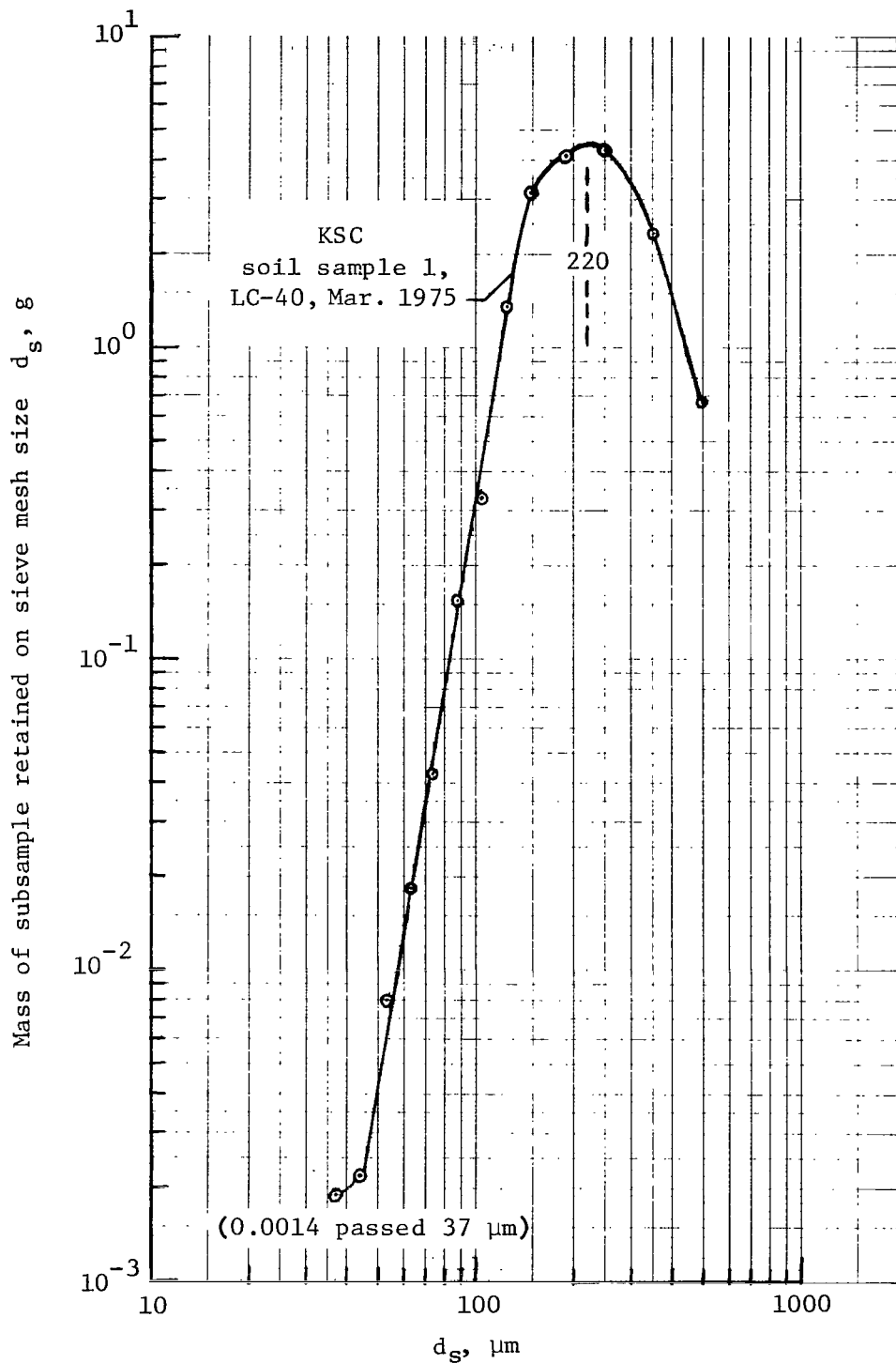
Figure 1.- Raw-mass-distribution data for KSC soil sample 1.
Gravimetrically determined after sequential sifting with
calibrated sieve screens. Logarithmic interval spacings
for $d_s \geqslant 149$ μm differ from that for $d_s < 149$ μm.
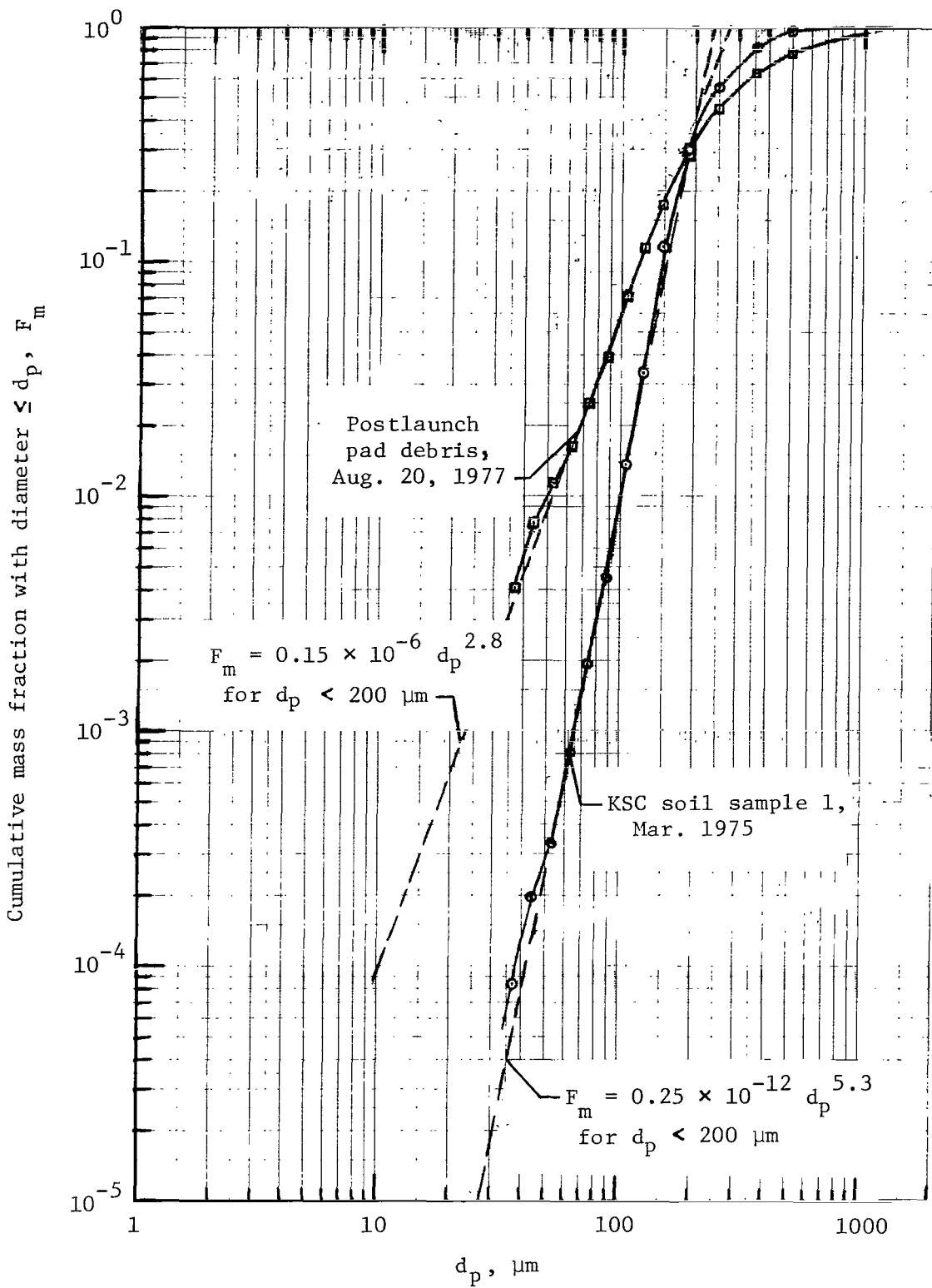
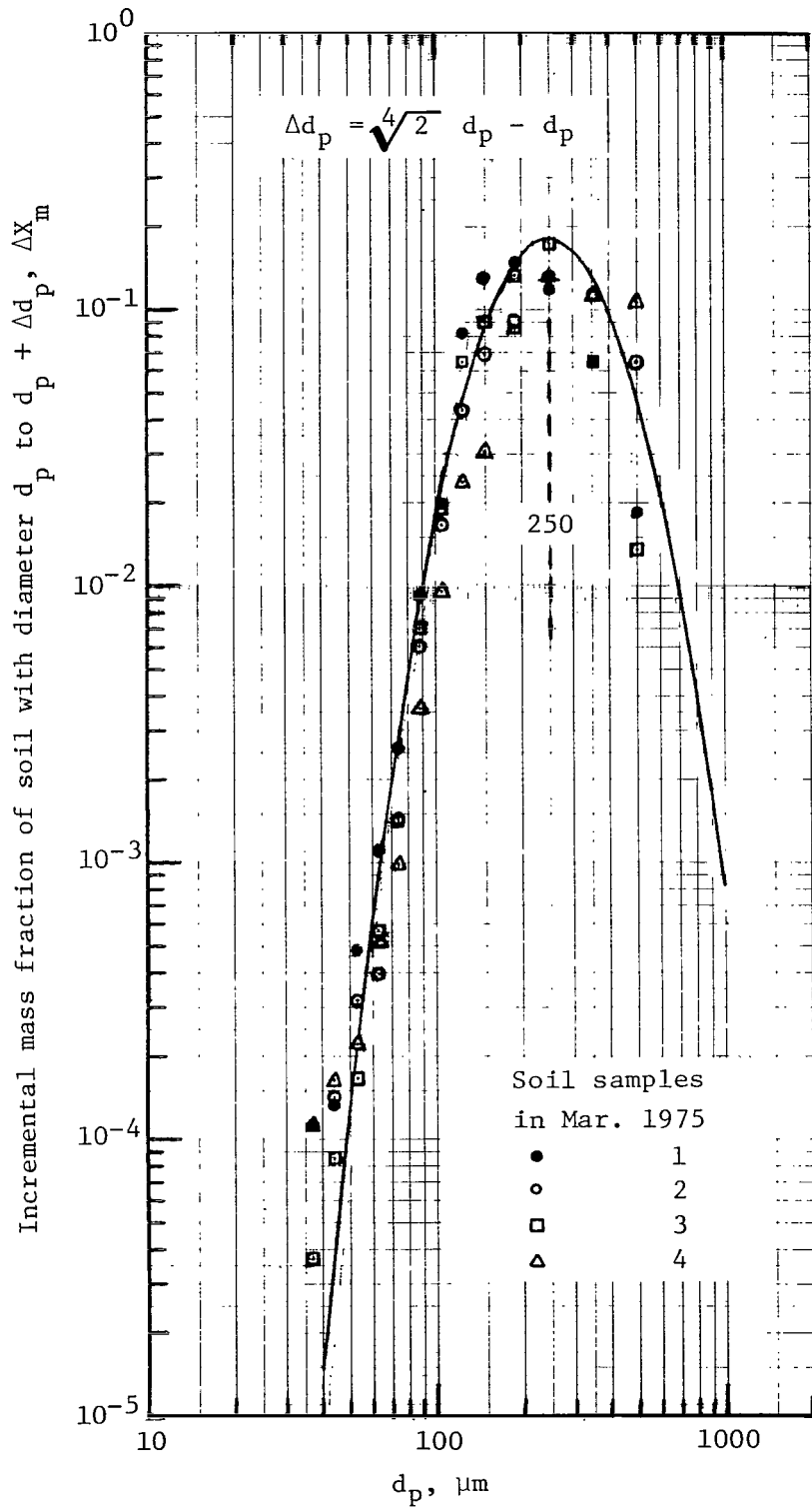Figure 2.- Normalized cumulative mass distribution of KSC soil sample 1 and a postlaunch-pad-debris sample.

$$\Delta d_p = \sqrt[4]{2} \ d_p - d_p$$

250

Soil samples
in Mar. 1975

●	1
○	2
▢	3
△	4

Figure 3.- Normalized differential mass distributions of
KSC soil samples 1 to 4 faired with a best-fit normalized
log-parabolic distribution function. Data on five largest-
size fractions were reduced to coincide with indicated
Δd_p-size interval.
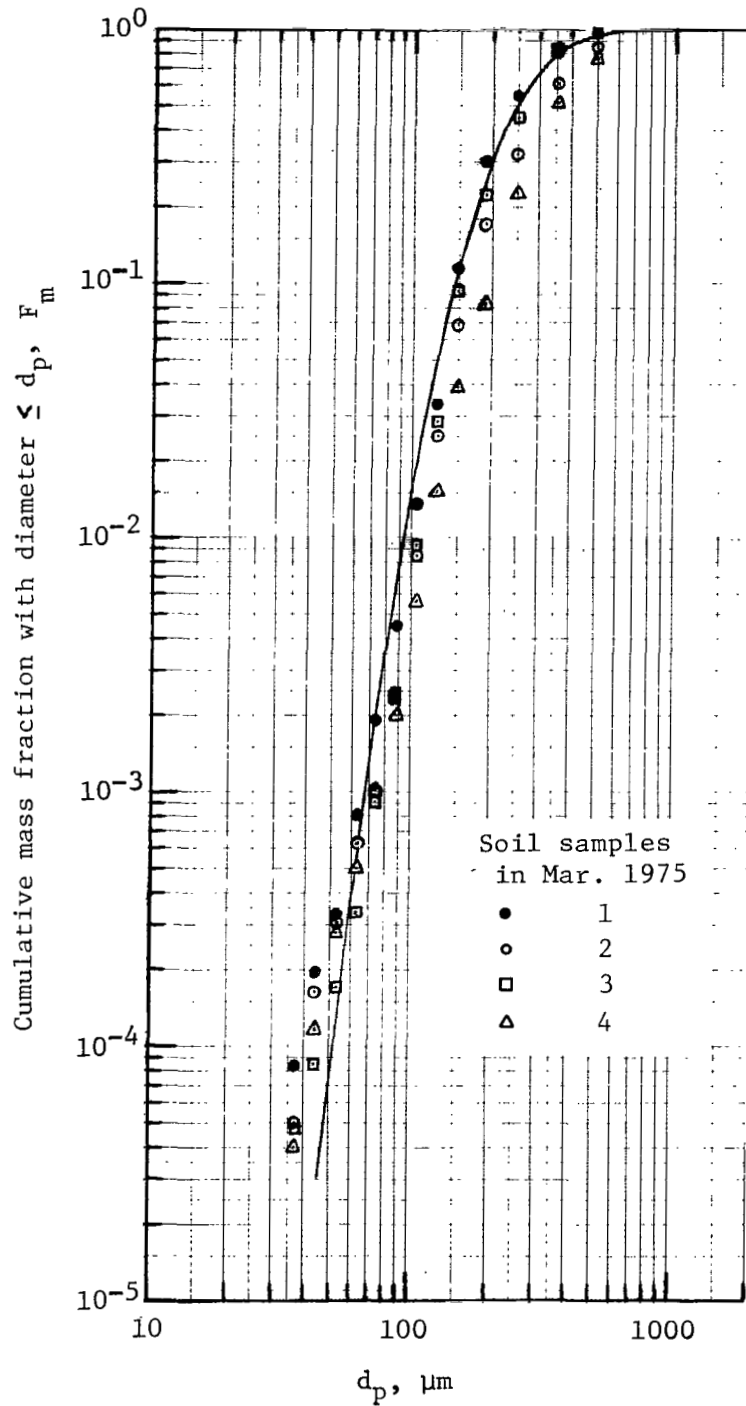
Figure 4.- Normalized cumulative mass distributions of
KSC soil samples 1 to 4 faired with integrated log-
parabolic distribution function deduced in figure 3.
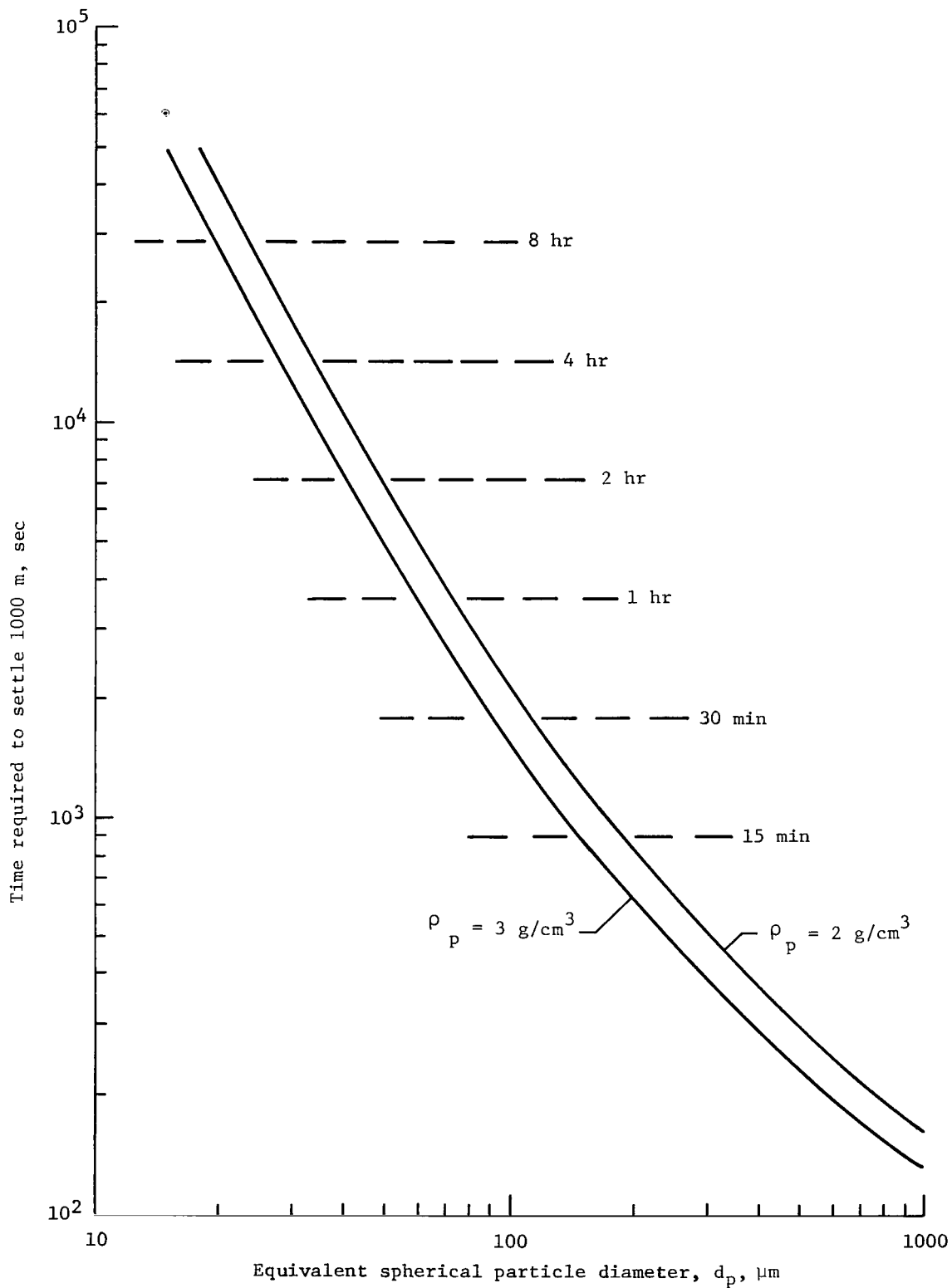
Figure 5.- Characteristic settling time required for spherical particles of various densities to fall 1000 m at terminal velocity in still air at 21°C, at a pressure of 1 atm.
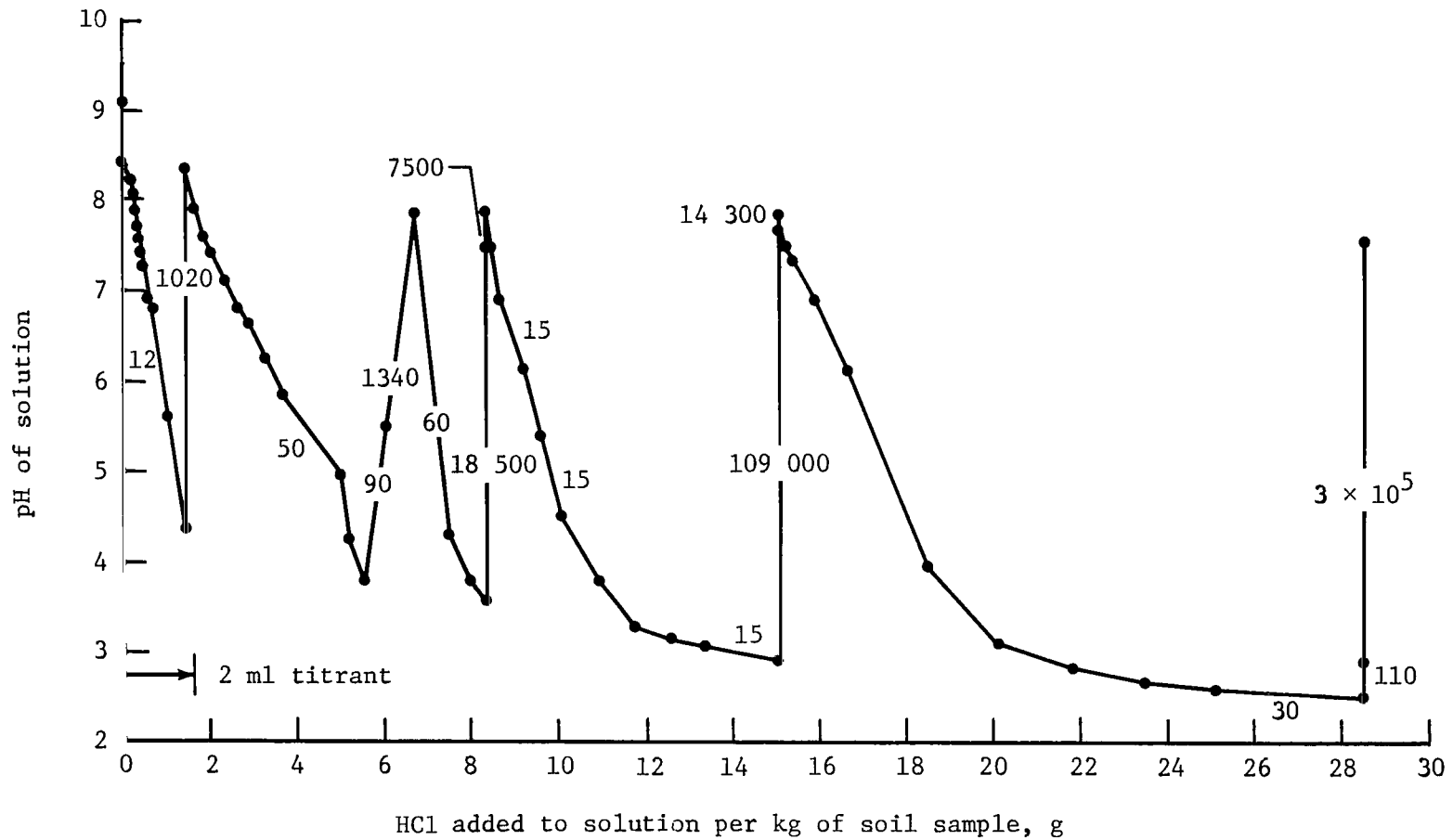
(a) 2.18 g of size fraction; 250 μm < d_p < 354 μm; in 100 ml of water.

Figure 6.- Results of time-sequenced titrations of slurried fractions of KSC soil sample 1 with 0.05 molar HCl. Each pH value was recorded after 10 min of stirring except where minutes are noted on graph.
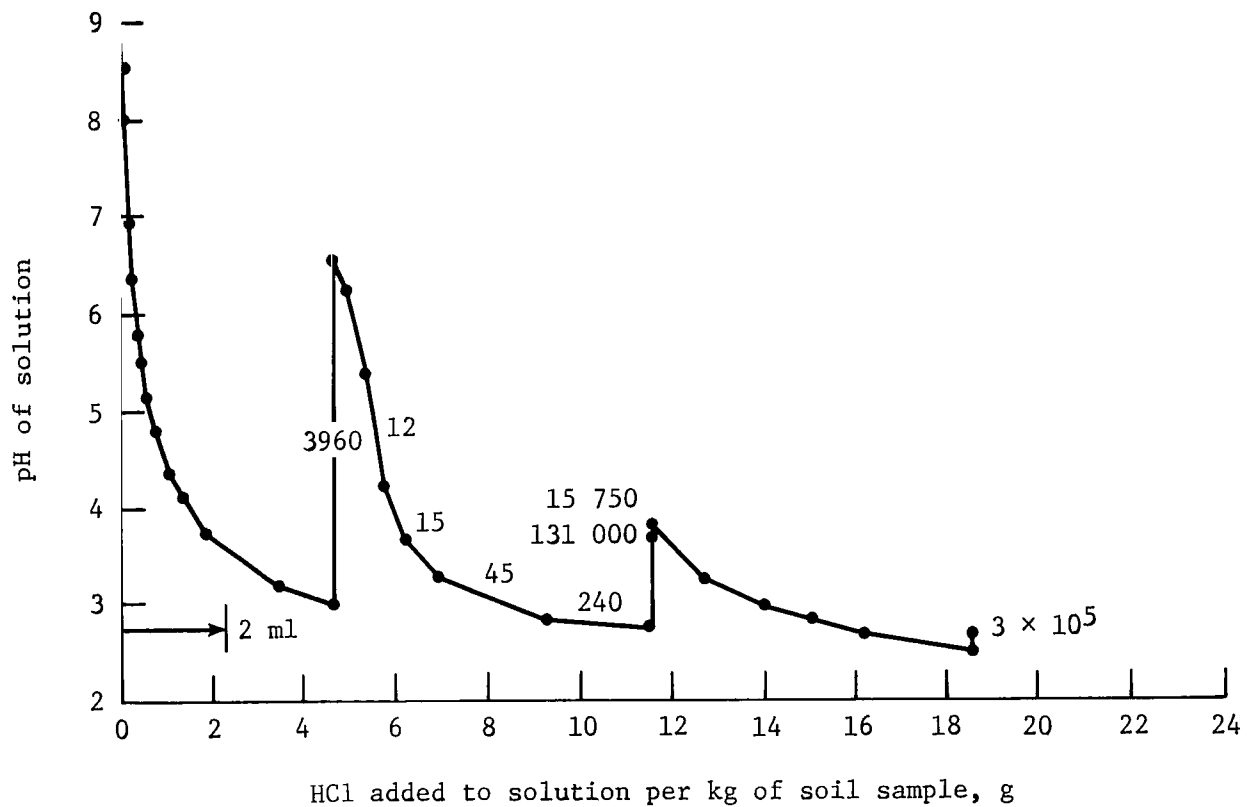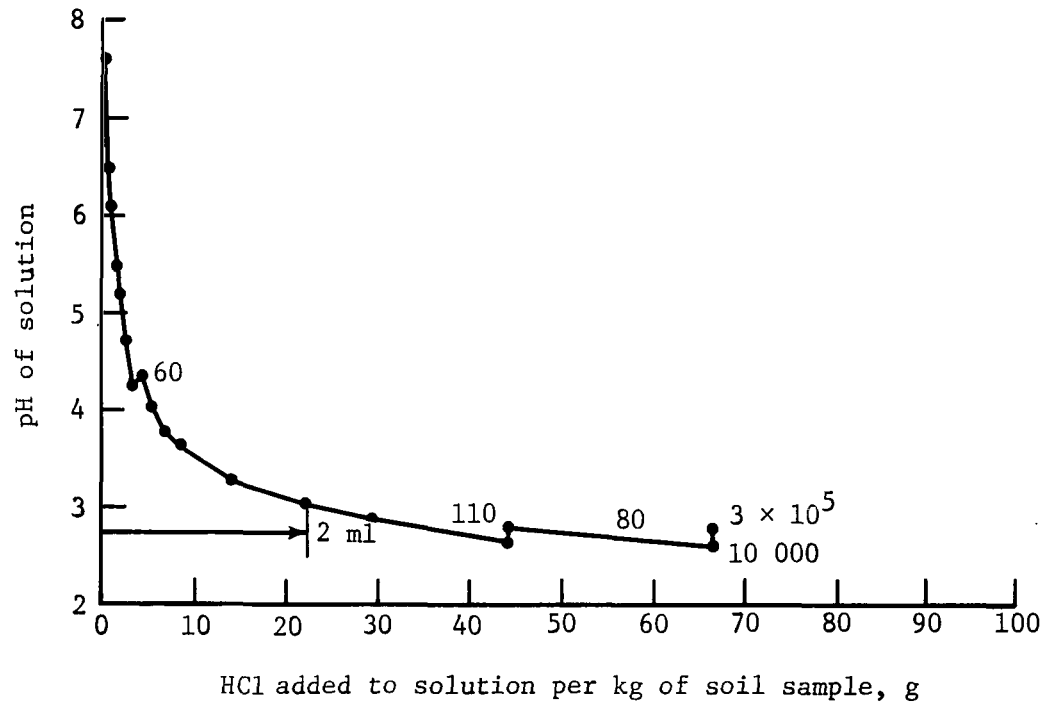
(b) 1.57 g of size fraction;   149 $\mu m < d_p < 190$ μm; in 100 ml of water.
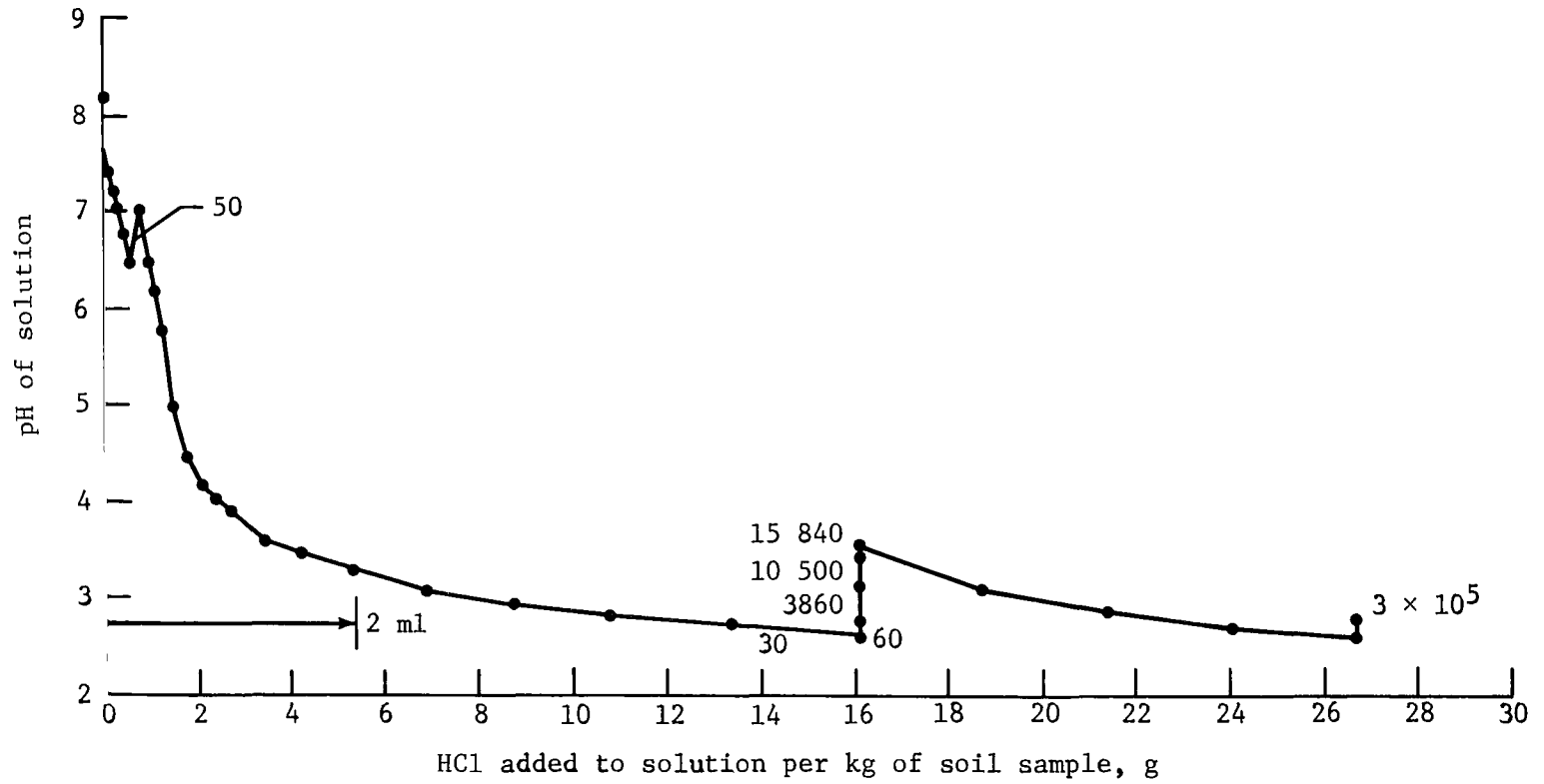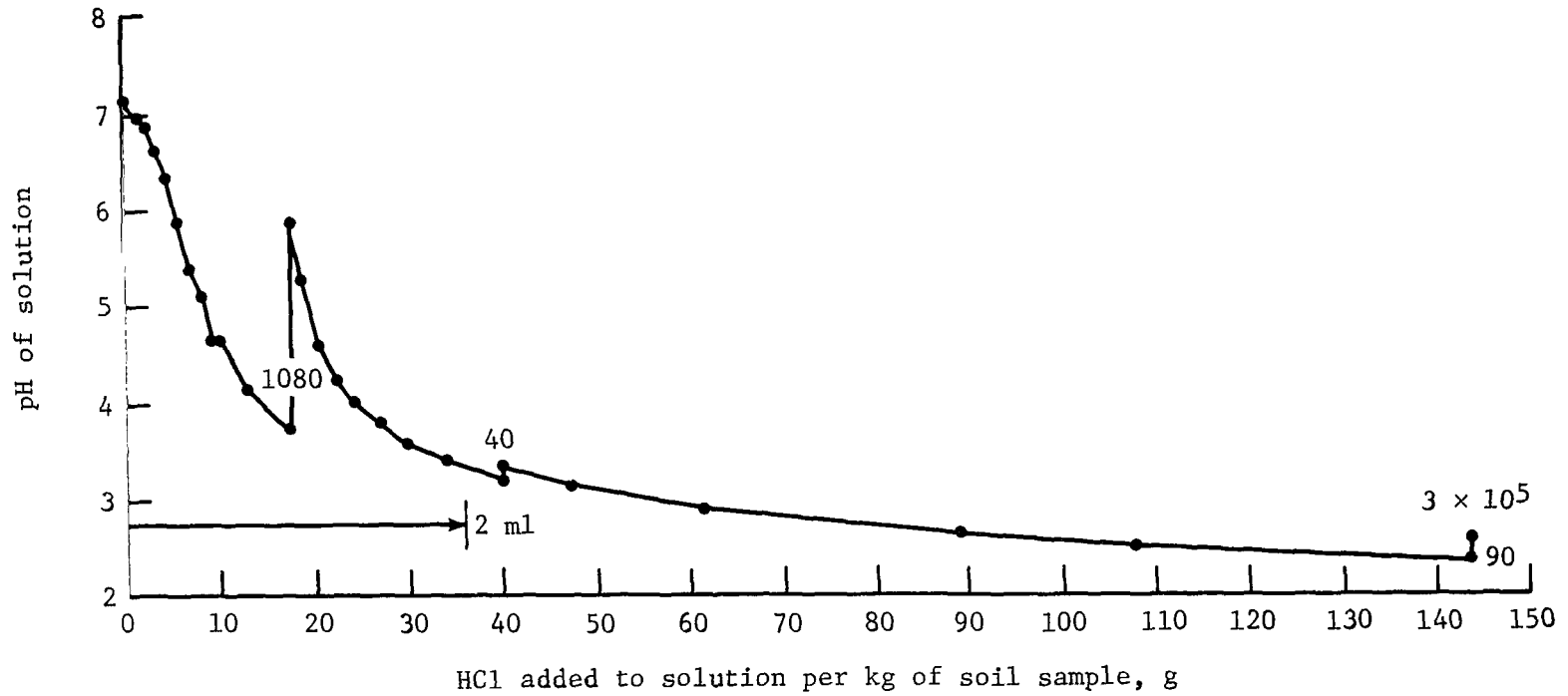
Figure 6.- Continued.

(c) 0.683 g of size fraction; 125 μm < d_p < 149 μm; in 100 ml of water.

Figure 6.- Continued.

(d) 0.165 g of size fraction; 105 μm < d_p < 125 μm; in 100 ml of water.

Figure 6.- Continued.

(e) 0.101 g of size fraction; 88 μm $< d_p <$ 105 μm; in 100 ml of water.

Figure 6.- Concluded.

1. Report No. NASA TP-2076	2. Government Accession No.	3. Recipient's Catalog No.
4. Title and Subtitle CHARACTERIZATION OF SOIL AND POSTLAUNCH PAD DEBRIS FROM CAPE CANAVERAL LAUNCH COMPLEX AND ANALYSIS OF SOIL INTERACTION WITH AQUEOUS HCl		5. Report Date October 1982
		6. Performing Organization Code 989-15-20-02
7. Author(s) G. L. Pellett, L. W. Spangler, R. W. Storey, Jr., and R. J. Bendura		8. Performing Organization Report No. L-15433
		10. Work Unit No.
9. Performing Organization Name and Address NASA Langley Research Center Hampton, VA 23665		11. Contract or Grant No.
		13. Type of Report and Period Covered Technical Paper
12. Sponsoring Agency Name and Address National Aeronautics and Space Administration Washington, DC 20546		14. Sponsoring Agency Code

15. Supplementary Notes

16. Abstract

Soil samples, collected near the Titan III Launch Complex 40 at Cape Canaveral, Florida, were fractionated and analyzed in order to assess the physical and chemical interactions of entrained soil with solid-rocket exhaust clouds. The sandy soil consisted primarily of quartz (silica) particles, 30 to 500 μm in diameter, and also contained seashell fragments. Differential and cumulative soil-mass size distributions are presented along with mineralogy, elemental compositions, and solution pH histories. About 90 percent of the soil mass consisted of particles >165 μm in diameter. Characteristic reaction times in aqueous HCl slurries varied from a few minutes to several days, and capacities for reaction under acidic conditions varied from >10 to >40 g HCl/kg soil, depending on particle size. Airborne lifetimes of particles >165 μm are conservatively <30 min, and this major grouping is predicted to represent a small short-term chemical sink for up to 5 percent of the total HCl. The smaller and more minor fractions, below a 165-μm diameter, may act as giant cloud condensation nuclei over much longer airborne lifetimes. Finally, the demonstrated time dependency of neutralization is a complicating factor; it can influence the ability to deduce in-cloud HCl scavenging with reaction and can affect the accuracy of measured chemical compositions of near-field wet deposition.

17. Key Words (Suggested by Author(s)) Environmental impact Hydrogen chloride Fractionation Chemical interactions Soil particles	18. Distribution Statement Unclassified - Unlimited Subject Category 45

19. Security Classif. (of this report) Unclassified	20. Security Classif. (of this page) Unclassified	21. No. of Pages 23	22. Price A02

National Aeronautics and
Space Administration

Washington, D.C.
20546

Official Business
Penalty for Private Use, $300

S

NASA

POSTMASTER: If Undeliverable (Section 158
Postal Manual) Do Not Return